

Pupil plane multiplexing for multi-domain imaging sensors

Roarke Horstmeyer^{*}, Gary W. Euliss, Ravindra A. Athale, The MITRE Corp.; Rick L. Morrison, Ronald A. Stack, Distant Focus Corp.; Joseph Ford, Univ. of California/San Diego

ABSTRACT

We describe an approach to polarimetric imaging based on a unique folded imaging system with an annular aperture. The novelty of this approach lies in the system's collection architecture, which segments the pupil plane to measure the individual polarimetric components contributing to the Stokes vectors. Conventional approaches rely on time sequential measurements (time-multiplexed) using a conventional imaging architecture with a reconfigurable polarization filter, or measurements that segment the focal plane array (spatial multiplexing) by super-imposing an array of polarizers. Our approach achieves spatial multiplexing within the aperture in a compact, lightweight design. The aperture can be configured for sequential collection of the four polarization components required for Stokes vector calculation or in any linear combination of those components on a common focal plane array. Errors in calculating the degree of polarization caused by the manner in which the aperture is partitioned are analyzed, and approaches for reducing that error are investigated. It is shown that reconstructing individual polarization filtered images prior to calculating the Stokes parameters can reduce the error significantly.

Keywords: multiplex, polarization, coded aperture, pupil plane, Stokes vector, PSF engineering

1. INTRODUCTION

1.1 Background and Motivation

Apart from containing spatial and spectral information, the electromagnetic radiation emanating from a particular scene also contains details regarding its polarimetric state. This polarimetric data can be particularly useful, for example, when attempting to distinguish manmade objects from natural objects. Surfaces that are made of metal, glass, and even minimally reflective materials like asphalt often exhibit a certain degree of polarization that obeys Fresnel's equations, while most natural vegetation does not¹. A polarimetric image can thus be regarded as an additional avenue through which threat detection and classification can be realized.

The polarization of an electromagnetic wave is often characterized by a set of four real numbers, known in vector form as the Stokes vector,

$$S = \begin{pmatrix} S_0 \\ S_1 \\ S_2 \\ S_3 \end{pmatrix}. \quad (1)$$

The first parameter S_0 is simply the total intensity, while the other three independent parameters are a scaled form of the Cartesian coordinates of the state of polarization's location on the Poincare sphere². One simple way to think about these last three parameters is as the comparison of light intensity in one polarization direction to that in another, orthogonal polarization direction. S_1 compares horizontal and vertical polarization, S_2 compares 45-degree and 135-degree polarization, and S_3 compares right and left circular polarization. The intensity in each of these directions can be measured by placing an appropriately aligned polarizer in front of a detector, blocking all but a certain polarization state of the light. If I_x represents the remaining intensity of the light after it passes through a polarizer aligned in a state x , then S becomes

^{*} E-mail: Horstmeyer@mitre.org

$$S = \begin{pmatrix} I_0 + I_{90} \\ I_0 - I_{90} \\ I_{45} - I_{135} \\ I_R - I_L \end{pmatrix}, \quad (2)$$

where the numerical subscripts represent the angle at which the polarizer is aligned, and R and L represent right and left circular polarization, respectively.

Several different quantities regarding the state of polarization can be derived once the Stokes vector is known, including the degree of polarization (DOP) and orientation angle of the major axis of the Poincare sphere (γ), given as

$$DOP = \sqrt{(S_1^2 + S_2^2 + S_3^2)} / S_0 \quad (3)$$

$$\gamma = \frac{1}{2} \tan^{-1}(S_2/S_1). \quad (4)$$

The degree of polarization is of particular interest in remote sensing and locating manmade objects in a natural setting, and it can be thought of as the distance from the origin to the state of polarization on the Poincare sphere. Calculating the DOP of a particular scene can yield object differentiation and possibly even surface orientation when reflected light is under observation³.

Conventional means of obtaining the polarization components required for computation of the Stokes vector are somewhat limited. Perhaps the most straightforward approach would include the use of a mechanically reconfigurable polarization filter or wave retarder^{4,5} and a sequential collection of images. This approach is relatively simple to implement, particularly for static scenes, but the need for a reconfigurable polarizer can add bulk and complexity, as well as latency. Alternatively, multiple images can be collected simultaneously with each image filtered by the appropriate polarization. Different architectural implementations of this approach can be conceived, including the use of four separate aligned and registered imaging systems, or a single aperture with a beam splitting mechanism and multiple focal plane arrays. In either case, the approach will tend to be bulky and will require sensitive alignment to be maintained. Alternatively, polarization diversity can be achieved in the focal plane by placing separately oriented filters over individual pixels⁶, at the price of losing resolution and reconfigurability. In this paper, we explore a more integrated and novel approach to polarimetric imaging through the utilization of the compact, folded optics imaging system developed by Tremblay et al.⁷. In addition to taking advantage of the lightweight, compact characteristics of the folded system, the approach described below does not rely on mechanically reconfiguring the polarizers in order to obtain the Stokes parameters.

1.2 Folded Camera System

The polarimeter described in this paper is based on an unconventional optical imager unique in its folded annular lens. The imaging system collects light through an annular aperture, reflects the light off of four curved surfaces, and forms an image on a sensor located on the back of the lens (see Figure 1). The design essentially takes the optical path of a conventional refractive zoom lens and folds it between these reflective rings, causing the focal length of the camera to lose its direct dependency on the physical length of the system. This leads to a point spread function (PSF) of the form,

$$I(r) = \left(\frac{1}{\lambda z}\right)^2 \left| (\pi a_2^2) \left[\frac{2J_1\left(\frac{ka_2 r}{z}\right)}{\frac{ka_2 r}{z}} \right] - (\pi a_1^2) \left[\frac{2J_1\left(\frac{ka_1 r}{z}\right)}{\frac{ka_1 r}{z}} \right] \right|^2, \quad (5)$$

which is essentially the scaled difference between two Jinc functions, or the PSFs of two circular apertures defined by the outer and inner diameters of the annulus. Optical power is moved from the central peak in a conventional circular aperture to the side lobes in an annular system, which causes some reduction of the optical transfer function for midrange frequencies. This reduction is further magnified in the case of the polarimeter described here, which is designed to obscure a given fraction of the annular aperture. Additional effects of segmenting the annular aperture will be discussed in more detail in the next section.

The folded imager used to construct the polarimeter has a four-fold design, consisting of an annular aperture and four asymmetric, computer optimized reflective concentric rings focusing light onto a 1600 x 1200 pixel CMOS sensor custom designed by Forza Silicon with a 3 μm pixel size. The whole system is roughly 8 mm thick including its casing. A 5 mm thick baffle is placed in front of the aperture to reduce stray light. The imager has an effective focal length of 22 mm and the outer diameter of its annular aperture is 30 mm. The central obscured region of the annular aperture is 26.7 mm wide, or 79% of the total aperture area.

2. POLARIMETER DESIGN

Two different approaches to obtaining the Stokes vector based on the folded, annular imaging system are described in this section. Each approach relies on segmenting the annular aperture and utilizes a fixed polarization mask. The difference between the two approaches is in the shuttering of the aperture to collect the individual components of polarization, and the processing required to then extract the Stokes parameters. The respective limitations and tradeoffs of the two approaches are analyzed, and a model is applied to examine their performance.

2.1 Three-Quarter Aperture Mask Design

In reference to the form of the Stokes vector described in Equation 2, there are six different intensity values that must be obtained to fully characterize the polarization state of a wave. However, by utilizing the general relationship

$$I_{tot} = I_0 + I_{90} = I_{45} + I_{135} = I_R + I_L, \quad (6)$$

only four separate measurements are necessary to estimate the Stokes vector image, as the original Stokes equation now becomes

$$S = \begin{pmatrix} I_0 + I_{90} \\ I_0 - I_{90} \\ 2I_{45} - S_0 \\ 2I_R - S_0 \end{pmatrix}, \quad (7)$$

where S_0 is the first Stokes parameter representing the total intensity.

To collect the four intensity values in Equation 7, four separate polarizers are placed in the annular aperture, each covering one quarter of its total area (see Figure 2). The polarizers are oriented to allow horizontal (0 degree), vertical (90 degree), 45 degree and right-circular polarized light to pass through the mask. The three linear polarizers were all cut from the same .75 mm thick film with a 38% transmission at peak (550 nm) wavelength. The circular polarizer consists of a linear polarizer combined with a quarter-wave retarder, having a 37% single pass transmission and oriented with the retarder facing away from the camera. A mask is then positioned to obscure three-quarters of the aperture and allow light to pass through only one of the four polarizers (Figure 2.a). In this approach, four separate polarization measurements can be taken by sequentially rotating either the position of the polarizers or the aperture mask 90 degrees at a time, capturing one image through each polarizer. Equivalently, a shutter could be configured to enable the four segments to be individually opened and closed. If the polarizers are rotated and the aperture mask is left stationary, then each image of the scene is captured through the same quadrant of the annular aperture. This approach is of little interest since it offers no real advantage over a conventional technique. Alternatively, if the polarizers are left stationary and the aperture mask is reconfigured to capture each image from a different quadrant of the aperture, then several issues arise regarding the changing PSF of the system (to be addressed later in this section).

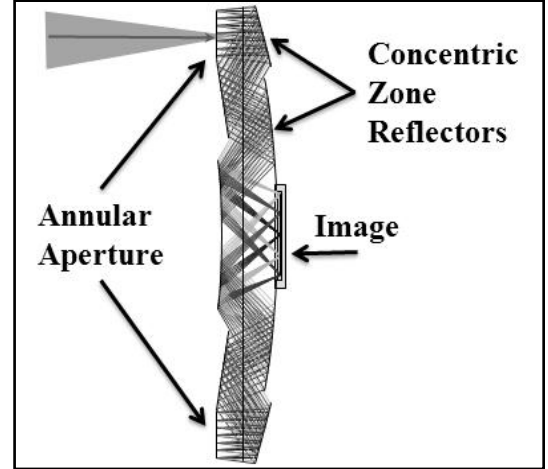


Figure 1: The folded imager (four-fold system) ⁷.

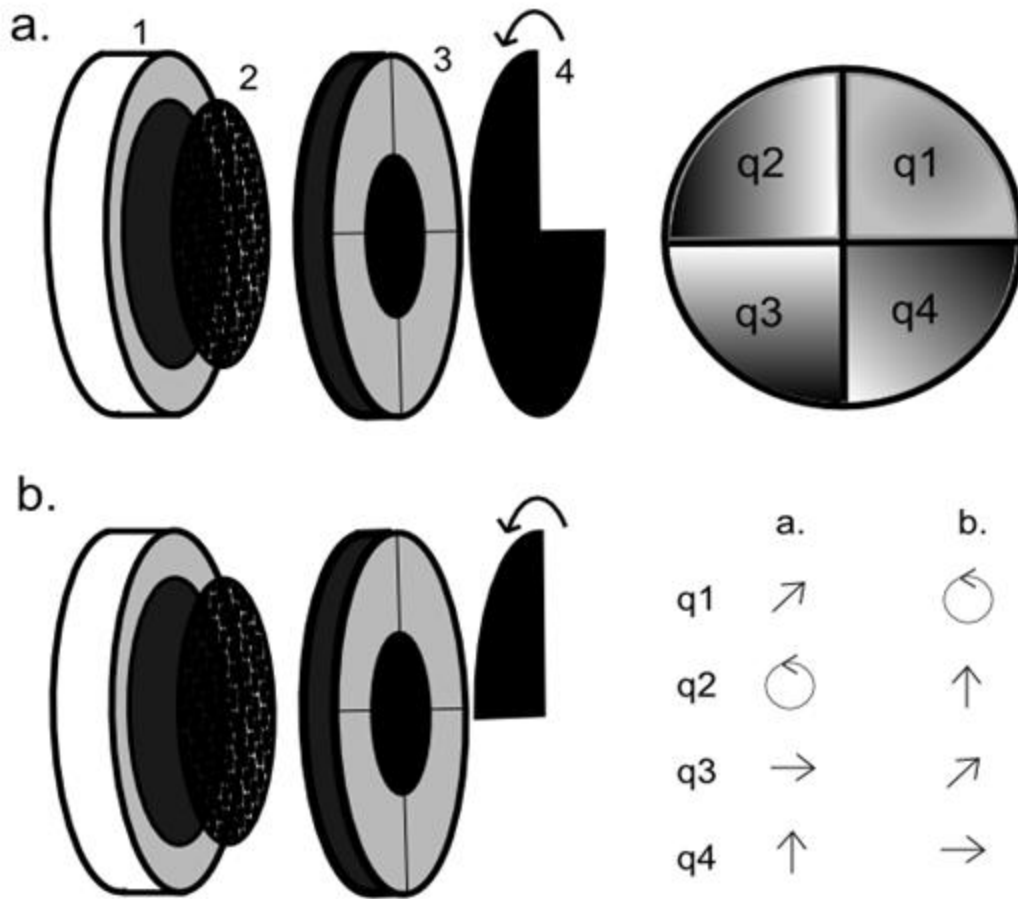


Figure 2: The general design for our polarimeter mask with the folded annular camera (1), the camera’s 5mm-thick baffle (2), the custom-built four polarizer arrangement (3), and an obscuring mask (4). Design (a) is the three-quarter mask design with a reconfigurable three-quarter aperture mask. Design (b) is a one-quarter mask design, also with a stationary polarizer arrangement and a reconfigurable mask. The table in the lower right designates which orientation of polarizer was used in which quadrant, with the circle representing right-circular polarization. Two different polarizer arrangements were designed to explore how the spatial orientation of the filters affects error in the calculation of Stokes vectors.

2.2 One-Quarter Aperture Mask Design

Instead of capturing one polarization state at a time as described in Section 2.1, a multiplexed approach can be applied that captures three out of the four polarization states in each exposure. The three-quarter aperture mask of the original approach is replaced with an aperture mask that obscures only one-fourth of the aperture as illustrated in Figure 2.b. Four separate images are again obtained, in which a different quadrant of the aperture (polarization state) is obscured for each image. Note that it is possible to design a polarimeter with a one-quarter aperture mask that permanently covers the same quadrant of the aperture, while the polarizer arrangement is rotated 90 degrees between images. However, this also requires physically reconfiguring the polarizers in some manner, which we want to avoid.

After capturing four images, each containing three different polarization states, a set of linear equations can be used to obtain the Stokes parameters. If I_p represents an exposure with the p -polarization quadrant obscured, then the vector

$$S = \begin{pmatrix} (2(I_c + I_{45}) - I_H - I_V)/3 \\ I_V - I_H \\ I_H + I_V - 2I_{45} \\ I_H + I_V - 2I_c \end{pmatrix} \quad (8)$$

describes the Stokes vector. Like Equation 6, this vector form takes advantage of the equality relationship between summed orthogonal polarization states. Furthermore, it works under the assumption that the measured intensities from each quadrant are separable and additive within the range of the sensor. The limitations of these assumptions will be examined in the next section.

3. ANALYSIS

Changing the pupil geometry will in general have an effect on the characteristics of the imaging system, and others have proposed and demonstrated partitioning apertures by polarization for different purposes⁸⁻¹². Some polarizer geometries are useful for extending depth of field⁸, while others can increase resolution in applications like microscopy^{9,10} and lithography¹¹. In our system, since each image is collected from a different region of the aperture, the PSF corresponding to each polarization component will in general be different. Furthermore, as the geometry of the four polarizers will also change the PSF, their specific arrangement in the aperture must be taken into account.

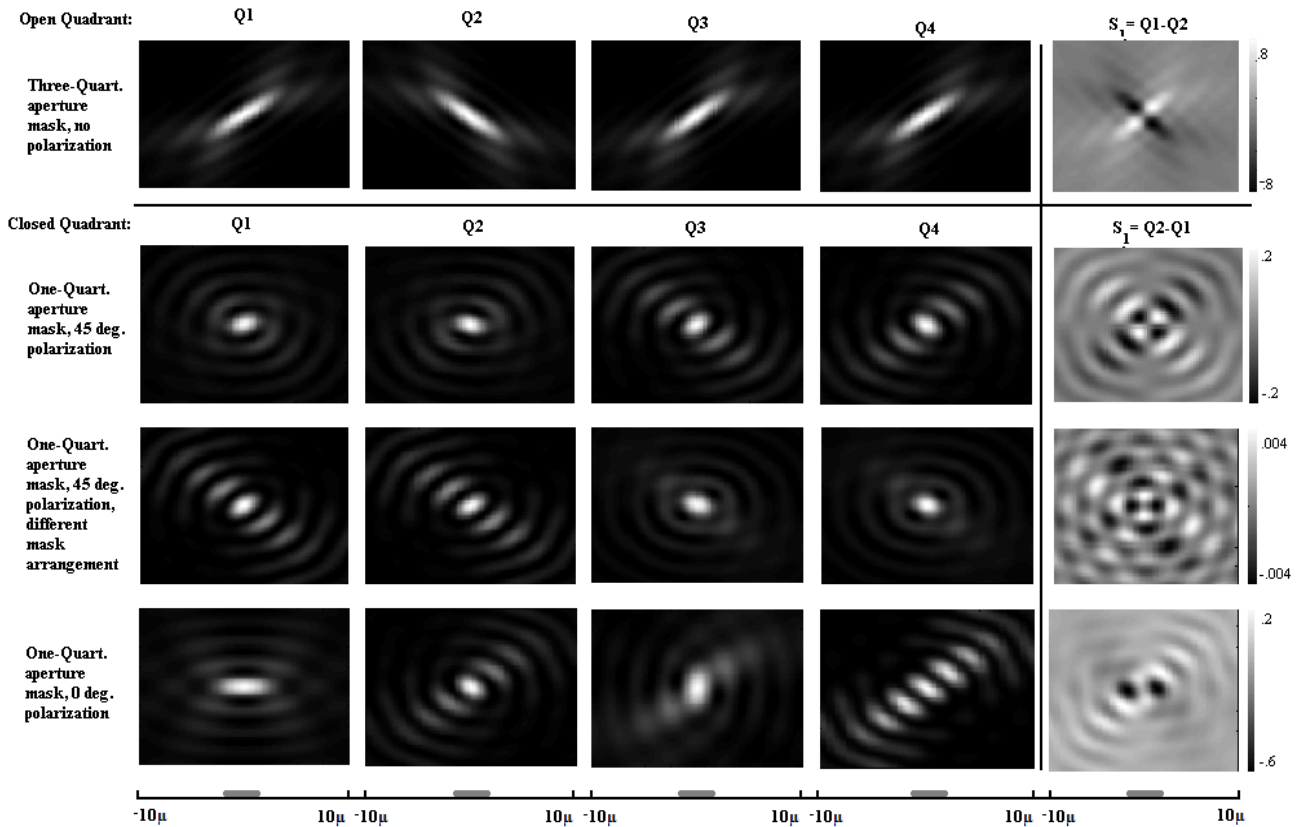


Figure 3: The various PSFs produced by the rotating mask design for the annular imaging system focused at infinity. The first four columns indicate which quadrant in Figure 2 remains clear (2.a) or blocked (2.b) and hence which polarization component (2.a) or components (2.b) are being imaged. The fifth column is the Stokes parameter S_1 , which is the difference between column Q1 and column Q2. The gray line along the spatial axis at the bottom of the image indicates the size of one pixel (3μ) in our system.

Figure 3 displays some different PSFs produced by the polarimeter. Each row contains the PSFs of a different aperture configuration, with the first four columns delineating the different mask orientations used to capture the four separate images used for Stokes vector calculation. Based on these results, the PSF is expected to span several of the 3μ pixels of our experimental system. The inconsistency in the PSF between polarizations will lead to errors in the calculation of Stokes parameters, indicating polarization when none is present. To illustrate, the first row in Figure 3 contains the four PSFs corresponding to each of the individual quadrants of the aperture. For unpolarized light, $Q_1 = Q_2$ and therefore $S_1 = 0$. But as Figure 3 shows, when Q_1 and Q_2 are collected through different quadrants of the annular aperture, $S_1 \neq 0$, resulting in an erroneous calculation of the Stoke's parameter. The effect is worse when collecting single quadrants sequentially than when the multiplex technique is applied simply because there is more variation between PSFs. However, the single quadrant approach has the advantage of a larger depth of field¹³. Since the full annular aperture exhibits a smaller depth of field than a conventional camera of similar NA at shorter object distances (approximately 24 mm at 2.5 m), this can be an important advantage.

The next three rows in Figure 3 display PSFs for the rotated one quarter mask system. Benefits of this multiplexed approach include an extended transfer function (along certain directions) and a threefold increase in light capture. However, to achieve these benefits one must pay a price in the increased computational complexity and higher degree of propagated error inherent in Equation 8. One other potential benefit, which depends on both the arrangement of the polarizers within the aperture as well as the polarization state of the scene being examined, is the possibility of minimizing the differences between the four PSFs.

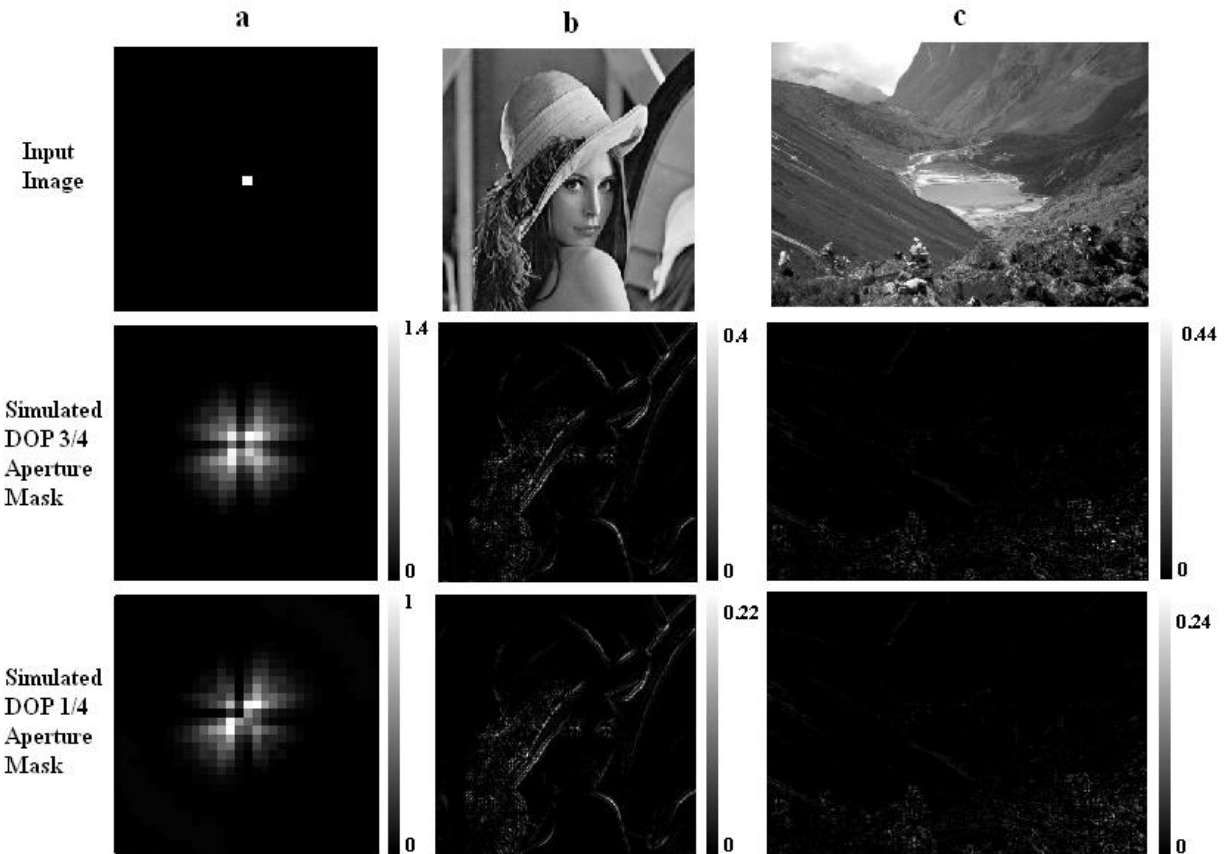


Figure 4: Three images are used to model the degree of polarization (dop) response for both the one-quarter and three-quarter aperture mask polarimeter designs. (Column a) The image and dop model measurements of a point source. (Column b) The image and dop model measurements for a portrait image. Note that the maximum dop for these two images are different, causing their display scales to differ. (Column c) The image and dop model measurements for a scenic image. Again, the scales on these two images are different.

Comparing the S_1 calculations for a 45-degree polarized scene, not only is the value nonzero, but the value is different for two different polarizer arrangements. This potential to engineer PSFs that combine or yield results with less error by changing the geometry of the polarimeter mask was not explored in detail in this experiment, but it does indicate the potential for optimizing the prototype mask design based on the task.

The problem with an inconsistent PSF between measured polarization states is that errors will be introduced in the calculation of Stokes parameters that will lead to a false degree of polarization. The significance of this problem can be examined by modeling the collection of polarization images through the partial apertures and calculating the Stokes parameters and subsequent degree of polarization. We begin by simulating the collection of polarization images of an unpolarized point source. Figure 4.a shows the apparent degree of polarization resulting from both the three-quarter and one-quarter mask approaches and determined using Equations 3, 7, and 8 for a single point source. Since the degree of polarization should be zero, any nonzero values represent erroneous polarization. If this same analysis is applied to an unpolarized image, erroneous polarization will also be indicated.

This is demonstrated in Figures 4.b and 4.c, where the degree of polarization is modeled for a detailed portrait and a natural scene at infinity, where no polarization has been assumed. Note that the erroneous polarization tends to appear primarily along boundaries between dark and light regions of the scene. As expected, the amount of erroneous polarization is significantly less for the quarter-mask approach in comparison to the three-quarter mask approach.

In the previous examples, no attempt has been made to reconstruct the images based on prior knowledge of the PSF before calculating the Stokes parameters. Doing so should remove some of the variations between images caused by the difference in PSFs. Figure 5 shows the results of applying a simple Richardson-Lucy algorithm to the same images shown in Figure 4. The erroneous polarization is still present, but has been substantially reduced. While the maximum error value for the post-processed images has increased, error tends to develop only in highly detailed areas, causing the total amount to decrease. This change is outlined in Table 1, which includes the maximum error value and the RMSE for each degree of polarization image.

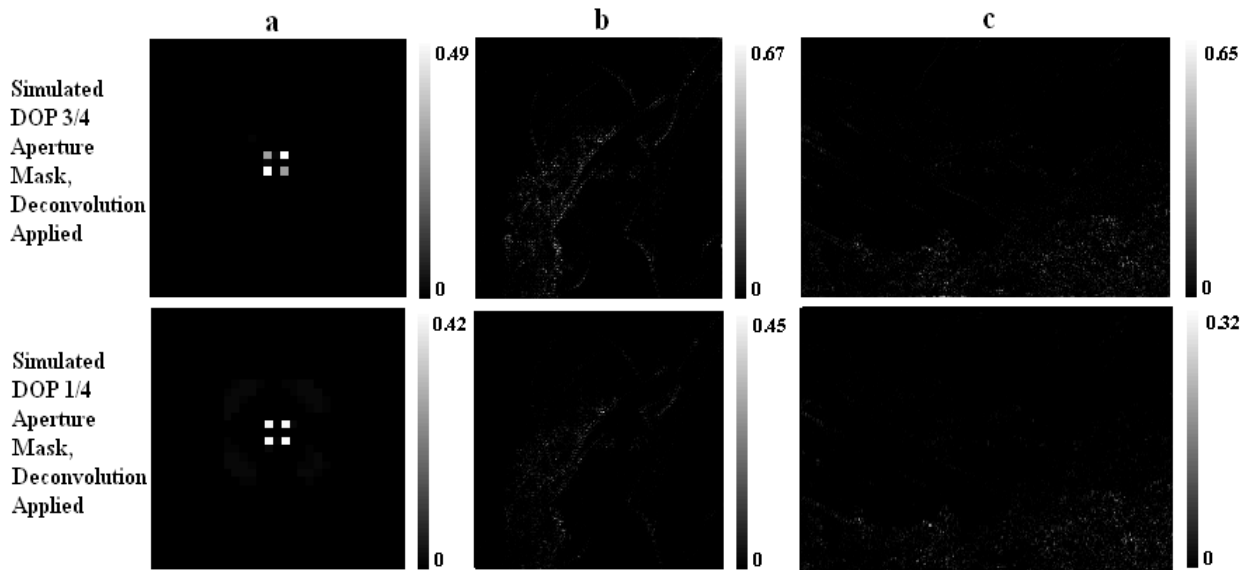


Figure 5: The dop measurements for the same three images in Figure 4, processed with the Richardson-Lucy algorithm before application of Equations 7, 8 and 3. (Column a) The reconstructed dop model measurements of a point source. (Column b) The reconstructed dop model measurements for a portrait image. (Column c) The reconstructed dop model measurements for a scenic image. The displays of these dop measurements are scaled to their respective maximums, as in figure 4.

We can also consider reducing the impact of the variation in PSFs by decreasing the effective resolution of the sensor, which can be simulated by binning pixels prior to calculating the Stokes parameters. This represents a tradeoff between resolution and polarization error, but may be considered acceptable for a given application. Since the average PSF generated by our masked system (Figure 3) spans approximately 3 pixels, reducing the detector resolution of our system by a factor of 3 reduces the error introduced into the degree of polarization calculation. Figure 6 shows the results of applying this technique to the same images in Figure 4.

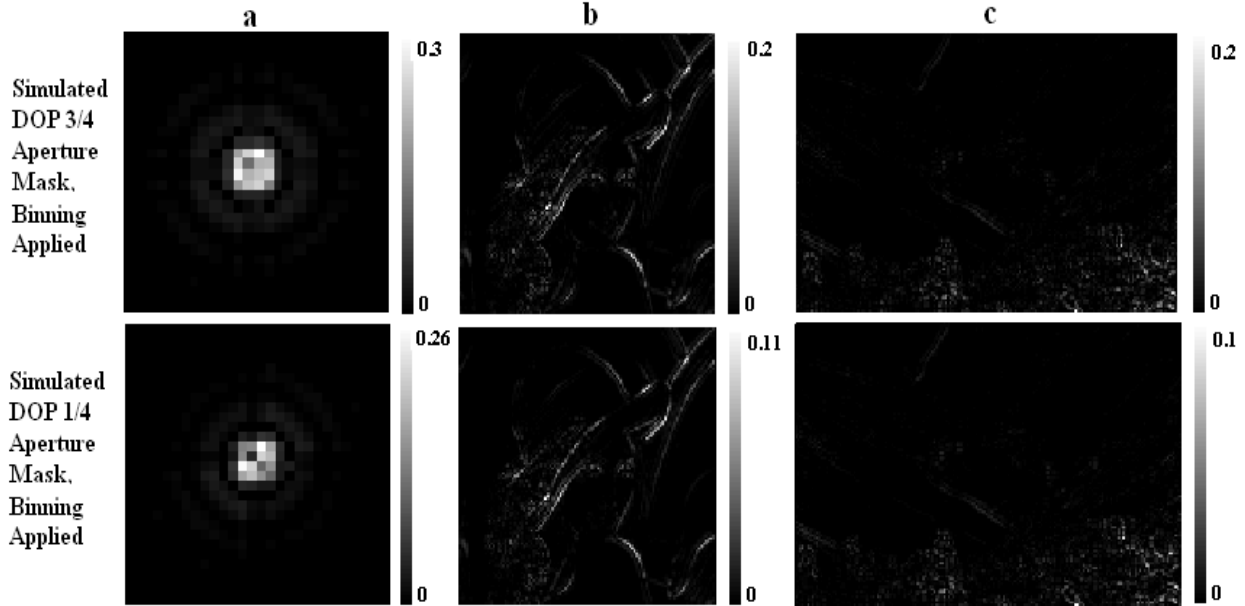


Figure 6: The dop measurements for the same three images in Figures 4 and 5, simulating a detector pixel size 3 times as large (9μ). (Column a) The dop model measurements of an unpolarized point source, which did not improve much compared to Figure 4 and became worse with respect to Figure 5. (Column b) The reconstructed dop model measurements for a portrait image. (Column c) The reconstructed dop model measurements for a scenic image. Again, note the scale change with respect to Figures 4 and 5.

	Point Source (max, RMSE)	Portrait Image (max, RMSE)	Landscape Image(max, RMSE)
$\frac{3}{4}$ mask, no processing	1.5288,0.0710	0.3976, 0.0087	0.4368, 0.0062
$\frac{3}{4}$ mask, Richardson-Lucy	0.4855, 0.0024	0.6673, 0.0070	0.6489, 0.0068
$\frac{3}{4}$ mask , binned	0.2921, 0.0027	0.1991, 0.0056	0.1921, 0.0031
$\frac{3}{4}$ mask, R-L and binned	0.0105, 0.0002	0.1486, 0.0011	0.0949, 0.0007
$\frac{1}{4}$ mask, no processing	1.0783, 0.0471	0.2152, 0.0044	0.2374, 0.0032
$\frac{1}{4}$ mask, Richardson-Lucy	0.4211, 0.0021	0.4453, 0.0027	0.3189, 0.0026
$\frac{1}{4}$ mask, binned	0.2549, 0.0008	0.1094, 0.0027	0.1005, 0.0016
$\frac{1}{4}$ mask, R-L and binned	0.0550, 0.0003	0.0700, 0.0003	0.0791, 0.0001

Table 1: The maximum degree of polarization value and the RMSE for the three different unpolarized scenes of Figures 4, 5 and 6. The first four rows are values for the three-quarter mask design, and the next four rows are values for the one-quarter mask design. “R-L and binned” represents images that were first processed with the Richardson-Lucy algorithm and then binned (there are no included images from this method). Note that values for the point source are limited to a 30×30 pixel array surrounding the point source.

Noting the scale change in Figure 6 with respect to the previous figures, decreasing the effective resolution of the sensor significantly decreases error introduced by inconsistent PSFs. Furthermore, two general trends are clear from the data in Table 1. First, the one-quarter mask multiplex design consistently exhibits a lower degree and amount of erroneous polarization measurement than the three-quarter mask design. Second, while applying prior knowledge or reducing resolution each work well individually, combining the two processes gets rid of erroneous polarization almost completely. Thus, implementing the multiplexed design with some simple image post-processing in combination with some slight resolution reduction almost completely mitigates error associated with sampling from different portions of the aperture.

When the camera is viewing a scene that exhibits a non-zero degree of polarization, the imaging characteristics of the three-quarter mask system will not change. The inconsistent PSFs used to calculate Stokes vectors will change in magnitude, but they will not change in shape. Thus, the prior knowledge algorithm and binning methods discussed above will remain effective at reducing error. The shape of the PSFs for the one quarter multiplexed system will change, however, as made clear in different PSFs in Figure 3. Prior knowledge of PSFs will be difficult to incorporate into an error minimizing algorithm, as the PSF of each pixel with a different polarization state will not be the same. Matching the pixel size more closely to the PSF is expected to be effective in reducing the polarization error, but this comes at the expense of resolution.

4. SUMMARY AND STATUS

In this paper, we have described two new approaches to polarimetric imaging based on a novel folded, annular imaging system. The approaches take advantage of the compact, lightweight characteristics of the folded imaging system and the unique characteristics of the annular aperture. In each approach, the four polarization components can be collected by simple zoned shuttering of the aperture without requiring physical reconfiguration of polarization filters. This feature represents an advantage over conventional approaches to polarimetric imaging requiring the polarizers to be reconfigured. We have analyzed the asymmetries that are introduced by partitioning the annular aperture and have shown how these asymmetries produce errors in the Stokes vector calculations, leading to erroneous polarization in the collected images. Techniques to reduce the polarization error have been suggested and explored, including reconstruction of polarization images with prior knowledge of the PSFs before calculating the Stokes vector. It was also shown that the polarization error can be reduced by matching the pixel size to the PSF, but at the expense of sacrificing resolution of the sensor.

We have built a prototype polarimetric imaging sensor based on the specifications and designs described in the paper, and have begun experiments with the system. Future work will include exploring additional approaches to reducing systematic polarization error, as well as experimental investigations with the prototype system.

REFERENCES

[1] Horvath, G., Gal, J., Labhar, T. Wehner, R., "Does reflection polarization by plants influence colour perception in insects? Polarimetric measurements applied to a polarization-sensitive model retina of *Papilio* butterflies," JEB 205, 3281-3298 (2002)

[2] Saleh, B.E.A. and Teich, M.C., [Fundamentals of Photonics], Wiley Series in Pure and Applied Optics, New Jersey, Ch. 6, 11 (2007)

[3] Chun, C.S.L., Sadjadi, F.A., "Polarimetric imaging system for automatic target detection and recognition," DTIC No. ADA392865 (2000)

- [4] Volin, C.E., Garcia, J.P., Sabatke, D.S., Dereniak, E.L., Descour, M.R., "MWIR Snapshot Imaging Spectrometer: Calibration and Imaging Experiments; Complete Imaging Stokes Polarimeter for The 3 - 5 Micrometer Spectral Band," DTIC No. ADA392949 (2000)
- [5] Volin, C. E., Garcia, J. P., Dereniak, E. L., Descour, M. R., Hamilton, T., and McMillan, R., "Midwave-Infrared Snapshot Imaging Spectrometer," *Appl. Opt.* 40, 4501-4506 (2001)
- [6] Chun, C.S.L., Sadjadi, F.A., "Polarimetric imaging system for automatic target detection and recognition," DTIC No. ADA392865 (2000)
- [7] Tremblay, E.J., Stack, R.A., Morrison, R.L., Ford, J.E. "Ultrathin cameras using annular folded optics," *Appl. Opt.* 46, 463-471 (2007)
- [8] Chi W., Chu K. and George, N., "Polarization Coded Aperture," *Optics Express* 14(15), 6634-6642 (2006)
- [9] Iglesias, I., Vohnsen, B., "Polarization structuring for focal volume shaping in high resolution microscopy," *Optics Comm.* Vol. 271, 40-47 (2007)
- [10] Neil, M.A.A., Juskaitis, R., Wilson, T., Laczik, J., "Optimized pupil-plane filters for confocal microscope point-spread function engineering," *Optics Letters* Vol. 25 No. 4 245-247 (2000)
- [11] Lindlein, N., Quabis, S., Peschel, U., Leuchs, G., "High numerical aperture imaging with different polarization patterns," *Optics Express* 15(9), 5827-5842 (2007)
- [12] Barnard, R., Gray, B., van der Gracht, J., Mirotznik, M., Mathews, S., "PERIODIC: state-of-the-art array imaging technology," *Proc. 45th annual ACM southeast regional conference*, 544-545 (2007)
- [13] Tremblay, E.J., Morrison, R.L., Stack, R.A., Ford, J.E., "Improving depth of field and reducing volume in annular folded imagers," *Adaptive Optics: Computational Optical Sensing and Imaging (OSA) Technical Digest CMB3* (2007)